Original Article
Synergistic antitumor effect of 20-(R)-Rg$_3$ combined with 5-fluorouracil on HCT-116 cell

Xiao-Lai Yang[1,4], Ting-Li Huang[1], Hong-Yi Cai[2], Xiao-Ling Huang[1,4], Zuo-Ren Yu[5], Xiong-Fei Yang[3], Yao-Chun Lv[3], De-Xi Guo[1,4]

Departments of [1]Pharmacy, [2]Radiotherapy, [3]Anorectal, Gansu Provincial People's Hospital, Lanzhou 730000, Gansu, PR China; [4]School of Pharmacy, Ningxia Medical University, Yinchuan 750004, PR China; [5]Research Center for Translational Medicine, Key Laboratory of Arrhythmias of The Ministry of Education of China, East Hospital, School of Medicine, Tongji University, 150 Jimo Road, Shanghai 200120, PR China

Abstract: 5-FU is widely used for the treatment of colorectal cancer (CRC), however, the severe cells toxicity of 5-FU is a principal obstacle of clinical application in CRC. 20(R)-ginsenoside Rg$_3$ (20-(R)-Rg$_3$, GRg$_3$), a monomer extracted from Panax ginseng roots, has significant anti-cancer effect. Up to now, the synergism of GRg$_3$ combination with 5-FU in CRC have not been reported. Therefore, this study aimed to explore the anti-cancer activity of GRg$_3$ in combination with a lower dose 5-FU and further identify the mechanism for inhibiting growth of cells. Cell viability and proliferation were detected by MTT assay and immunofluorescence with the antibody of ki-67. Apoptosis were tested by AnnexinV/PI assay and TUNEL. Flow cytometry was performed to evaluate cell cycle arrest. The expression of apoptotic-relate proteins were determined by using Western blot analysis. Our results demonstrated that co-treatment worked synergistically and more effectively than either drug alone in decreasing viability in HCT-116 cells. 5-FU and GRg$_3$ together exhibited greater cell cycle arrest in the S and G$_1$/G$_0$ than alone treatment. Furthermore, two-drug combination significantly down-regulated the expression of anti-apoptosis related proteins Bcl-2 and Bcl-xl and up-regulated significantly the expression levels of Bax, P53, cleaved-PARP and cleaved-caspase-3. Based on these data, we conclude that lower concentrations of 5-FU and GRg$_3$ used in combination produce a synergistic anti-cancer effect that is mediated by apoptosis through a mitochondrial pathway and arrest cells at S and G$_0$/G$_1$ phase. Collectively, Combination of 5-FU and GRg$_3$ could be regarded as a promising therapy for controlling the growth of CRC cells.

Keywords: 20-(R)-Rg$_3$, 5-FU, HCT-116 cells, anti-cancer effect, synergism

Introduction

Colorectal cancer (CRC) is one of the most commonly diagnosed malignancies and the third most common cause of cancer-related death in worldwide [1]. Surgical resection, chemotherapy or radiotherapy remains the mainly established curative treatment for CRC [2]. Although chemotherapy is often used as a main regimen in the treatment of CRC, severe toxicity represents a major obstacle in cancer therapy.

5-Fluorouracil (5-FU), which is a classical chemotherapy agent, was synthesized by Heidelberger and his colleagues at the University of Wisconsin in 1957 [3]. 5-FU and calcium folinate (CF) have been regarded as the first line regimen for treating CRC over several decades [4-6]. However, the clinical use of 5-FU on colorectal cancer is limited by serious side effects such as nausea, vomiting and myelosuppression when it was used at the therapeutic dose [7]. Therefore, an effective anti-cancer agent with minimal side effects is urgently needed for colorectal cancer therapy. Over the years, natural products have been discovered to be more effective than cancer drugs because of their multi-targeting and low toxicity properties [8-11].

20(R)-ginsenoside Rg$_3$ (20-(R)-Rg$_3$, GRg$_3$) (**Figure 1**), a bioactive extract of Panax ginseng, has significant anti-cancer effects *in vitro and in vivo* [12-15]. Xie's research showed GRg$_3$

Figure 1. Chemical structure of 20-(R)-Rg₃.

20-(R)-Ginsenoside Rg3
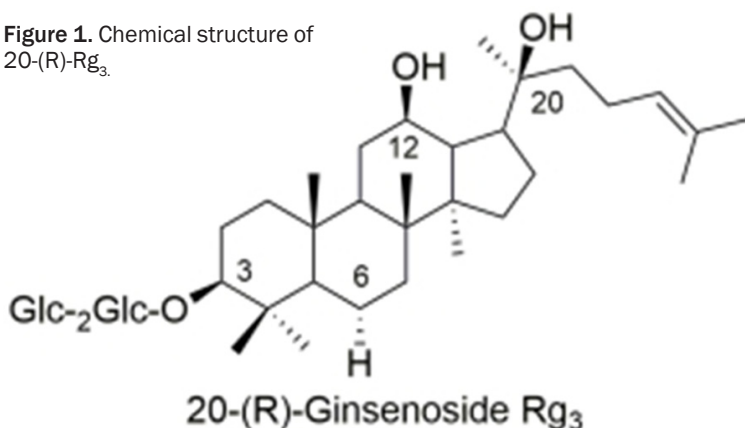
obviously inhibited cell viability, induced apoptosis and inhibited PI3K/Akt signaling pathway on A549, H23 cells [16]. Its anti-angiogenesis along with anti-cancer effects have been shown in several cancers [17-19]. Sun et al. demonstrated the role of GRg₃ in reduction of the intracellular ROS level and activation of apoptosis through regulation of apoptosis-associated proteins in Lewis lung carcinoma (LLC) [20]. Bo-Min Kim et al. suggested that GRg₃ induced apoptosis in breast cancer (MDA-MB-231) cells by blocking NF-κB signaling via inactivation of ERK and Akt as well as destabilization of mutant P53 to achieve [21]. Kim BJ's study showed that inhibition of GRg₃ on the growth of gastric cancer HEK293 cells may be related to the blockade of TRPM7 channel activity [22]. GRg₃ also has been reported to restrain liver cancer metastasis in nude mice, the mechanism may be related to regulating expression of nm23 and CD44. In addition, GRg₃ was found to prevent the suppression of BMP-2/BMPR1A/Runx2 signals induced by DEX both in GIOP rats and primary osteoblasts [23]. Although a large number of studies shown that GRg₃ has low toxicity and high efficiency characteristics in some tumors treatment, the investigations about GRg₃ on colorectal cancer therapy had been reported sporadically [24-27]. Up to now, the synergism of GRg₃ combination with 5-FU in CRC have not been reported *in vitro*.

Generally, Ginsenosides are very poorly absorbed following oral administration *in vivo* [28, 29]. Qian research reported that oral 100 mg/kg, the bioavailability of GRg₃ in rats was only 0.97%-1.15% [30]. Pharmacokinetic Studies conducted in past years showed that most of the GRg₃ was tested in the colon after oral administration [31]. One of the reasons of the poor bioavailability of GRg₃ is that it may be metabolized by colonic micro flora. GRg₃ may have a natural colon-targeting feature that may be of therapeutic interest in CRC.

Based on anti-cancer and pharmacokinetic properties of GRg₃, we suppose that when GRg₃ and 5-FU were used on CRC in combination *in vivo*, their toxicity would not be induced, and moreover their effect may improve treatment outcomes in a manner that is not associated with overt toxicity. In the present study, we explored the potential synergistic efficacy of 5-FU combined with GRg₃ and its possible mechanism of synergism in HCT-116 cells *in vitro*.

Materials and methods

Materials

Dulbecco's modified Eagle's medium (DMEM) purchased from M&C gene technology (Beijing, China), fetal bovine serum (FBS) and penicillin/streptomycin purchased from Life Technologies. The following antibodies: Bcl-xl, Bcl-2, Bax, cleaved caspase-3, cleaved PARP, P53 and β-actin (sc-47778) were purchased from Santa Cruz Biotechnology (Santa Cruz, CA, U.S)

Cell culture

Human HCT-116 cells, isolated from male patients suffering from colon cancer, were provided from Professor Zuoren Yu, Research Center for Translational Medicine, Key Laboratory of Arrhythmias of the Ministry of Education of China, East Hospital. DMEM (MACGENE) medium containing penicillin and streptomycin (100 mg/L) (Life Technologies) and 10% FBS (Gibco) at 37°C in a humidified environment with 5% CO_2 was applied for cell culturing.

Drug and agent preparation

5-FU and calcium folinate (CF) were purchased from Sigma (MO, USA), dissolved in PBS (50 mMol/L), and the solutions were stored at
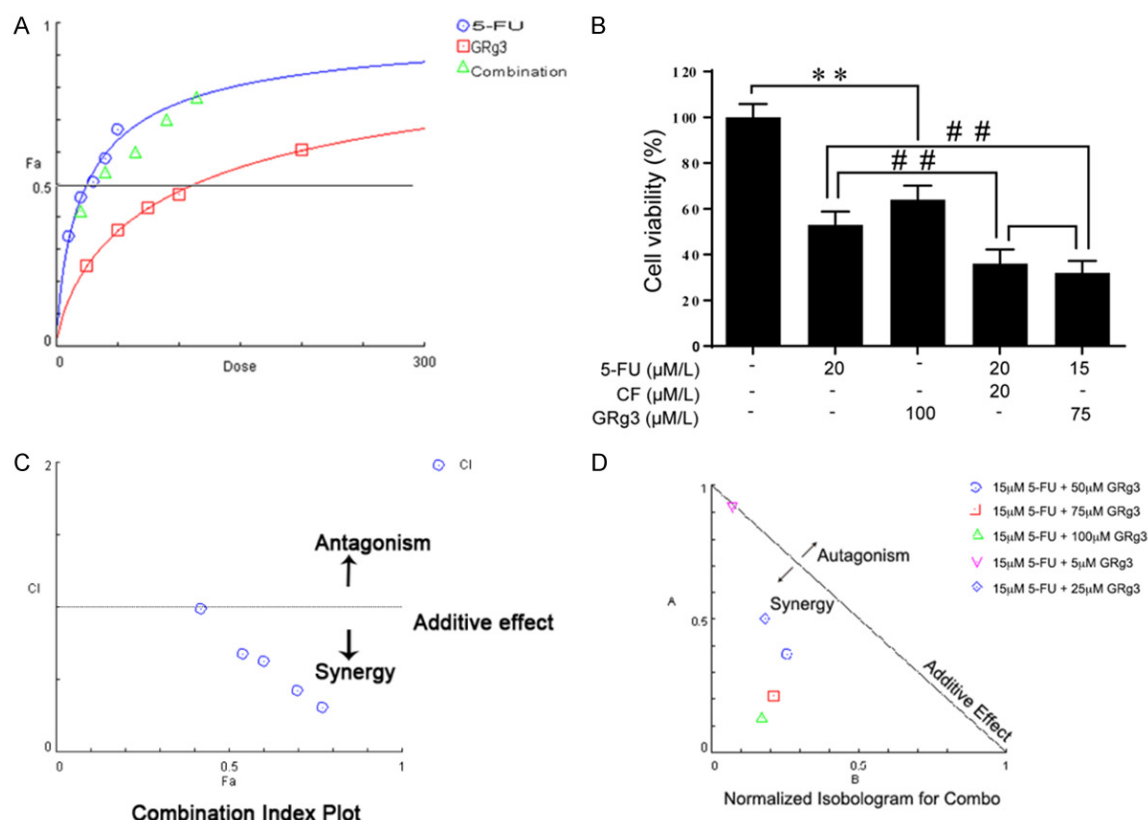
Figure 2. Effect of 5-FU and GRg$_3$ on the cell viability of HCT-116 cells was determined by MTT assay. A. Dose-effect curve for treatment with 5-FU (10, 20, 30, 40, 50 μM), GRg$_3$ (25, 50, 75, 100, 200 μM), 5-FU (20 μM) + CF (20 μM) or 5-FU (15 μM) + GRg$_3$ (5, 25, 50, 75, 100 μM) for 48 h. B. The cell viability of cells were measured by MTT when treated with 20 μM 5-FU, 100 μM GRg$_3$, 20 μM 5-FU + 20 μM CF or 15 μM 5-FU + 75 μM GRg$_3$ for 48 h. Combined treatment resulted in significant proliferation inhibition of HCT-116 cells, more than that by either drug alone (**P < 0.01, ##P < 0.01). C. The CI value was determined by using CompuSy software. CI < 1 indicates synergism, CI > 1 indicates antagonism, CI = 1 indicates summation. D. Effect of antagonism: the diagonal line represents the iso-effect line of additive. Points above this line indicate antagonism, and points below this line indicate synergy. All data are presented as mean ± s.e.m. (n = 5). *P < 0.05, **P < 0.01, compared with control group. #P < 0.05, ##P < 0.01, compared with 5-FU.

-20°C. GRg$_3$ (99.6% purity) was obtained from Suzhou star-ocean Jinsen Pharmaceutical Company (Suzhou, China). GRg$_3$ was dissolved in dimethylsulfoxide (DMSO) in a 100 mM stock solution and stored at -20°C. Aliquots of stock solution were added directly to the culture media.

Cell viability assay

The cytotoxicity of 5-FU and GRg$_3$ were assessed by MTT assay, which measures the inhibitive activity of viable cells. Cells were cultured in 96-well plates at a density of 4 × 10^3 cells/well overnight. Then cells were treated with various concentrations of 5-FU (10, 20, 30, 40, 50 μM), GRg$_3$ (25, 50, 75, 100, 200 μM) alone, 5-FU (20 μM) plus CF (20 μM) or

5-FU (15 μM) plus various dose of GRg$_3$ (5, 25, 50, 75, 100 μM). After drugs exposure for 48 h, 3-(4, 5-dimethylthiazol-2-yl)-2, 5-diphenyltetrazolium bromide (MTT) was freshly prepared and added to each well at a final concentration of 5 mg/ml. After incubation for 4 h, formazan crystals dissolved in 100 μl of DMSO, and the optical density was read by Spectra M5 (Molecular Devices, U.S.) at 490 nm. The concentrations required to inhibit growth by 50% (IC$_{50}$) were calculated from Dose-effect curves using the Bliss method. The data were analyzed by CompuSyn software with the results showed as combination index (CI) value according to the median effect principle, where CI < 1, = 1, and > 1 indicate synergism, additive effect, and antagonism, respectively [32]. Similar to the CI mode, the Isobole method
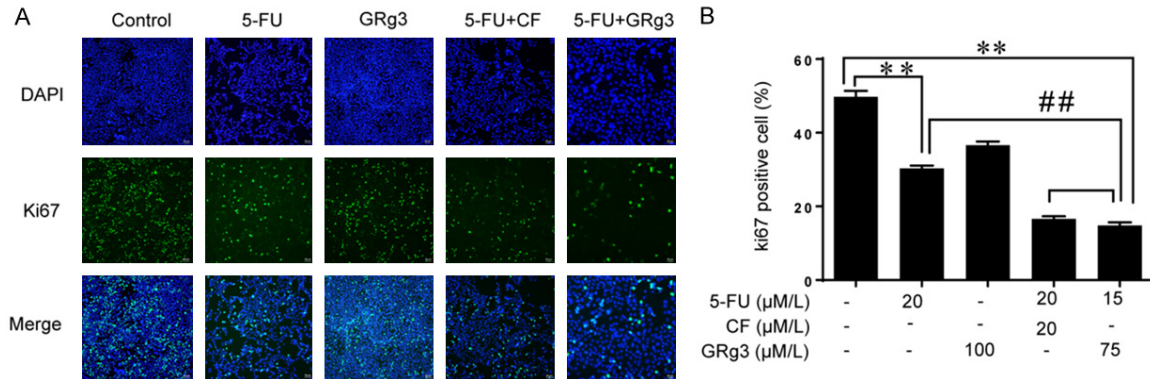
Figure 3. Immunofluorescence staining of Ki67 on HCT-116 cells. A. Anti-Ki67 antibody was detected using FITC conjugated secondary antibody (green) and nuclei were counter stained with DAPI (blue). The positive rate of Ki67 on HCT-116 cells increased along with the combination of 5-FU and GRg$_3$. B. Quantitative analysis of the ratio of Ki67 positive cells in all groups. All data are presented as mean ± s.e.m. (n = 3). *P < 0.05, **P < 0.01, compared with control. #P < 0.05, ##P < 0.01, compared with 5-FU.

requires the determination of dose-response relationship of the combination and it individual components independently to assess if synergism exists. The isobole is an iso-effect curve, in which a combination of components (A or B) at different dose levels is represented on the graph, the axes of which represent the dose-axes of individual component to reach the same effect. The equation for the isobologram-as follows: $CI = (D)_1/(Dx)_1 + (D)_2/(Dx)_2$, $(Dx)_1$, $(Dx)_2$ indicate the concentration of 5-FU or GRg$_3$ required to inhibit a given level of cell growth, and $(D)_1$ and $(D)_2$ are the concentrations of 5-FU or GRg$_3$ necessary to produce the same effect in combination, respectively.

Immunofluorescence staining of Ki-67 on HCT-116 cells

After washing with PBS, cells grow on coverslips were fixed with 4% paraformaldehyde (PFA) (Sigma Co.) for 30 min. Cells were then permeabilized with 0.1% Triton X-100 (Sigma Co.) for 5 min. After being blocked with 5% BSA for 1 h at room temperature, cells were incubated with immunofluorescence-anti-Ki67 (ab-15580, 1:500) at 4°C overnight. Then the slides were incubated with anti-rabbit secondary antibody for 2 h and then washed with 1 × PBS for 5 minutes. Nuclei stained with (4',6-dia-midino-2-phenylindole) DAPI (Sigma Co.) for 10 min. Images of immunofluorescence-stained HCT-116 cells were captured using fluorescence microscope (DMI3000B, Leica, Germany), and merged images were formed using Adobe Photoshop CS6.

Apoptosis assay using annexin V-FITC/PI staining

Cell apoptosis was detected using Annexin V-FITC/PI kit (BB-4101-3, Bestbio, China). Briefly, Cells seeded in 6-well tissue culture plates and treated with the test medium. After incubated for 48 h, cells were harvested and washed twice with cold 1 × PBS. Then resuspended in 400 μl binding buffer and stained with 5 μl each of Annexin V-FITC and 10 μl propidium iodide (PI) solution for 15 min at room temperature in the dark. The cells were analyzed immediately after staining by Flow cytometry.

TUNEL assay

Apoptotic cells were evaluated by TUNEL assay using *In situ* Cell Death Detection Kit, TMR red (Roche, Mannheim, Germany), according to the manufacturers' instructions. HCT-116 cells were fixed with 4% PFA for 15 min at room temperature and permeabilized using 0.1% Triton X-100 for 10 min. Nuclei stained with DAPI for 5 min. Cells were observed using a fluorescence microscope (DMI3000B, Leica, Germany). HCT-116 cells counted with Image J software.

Cell cycle analysis

Cell cycle distribution was detected by Flow cytometry. Cells were seeded in 6-well tissue culture plates and treated with drug-containing medium: 20 μM 5-FU, 100 μM GRg$_3$, 20 μM
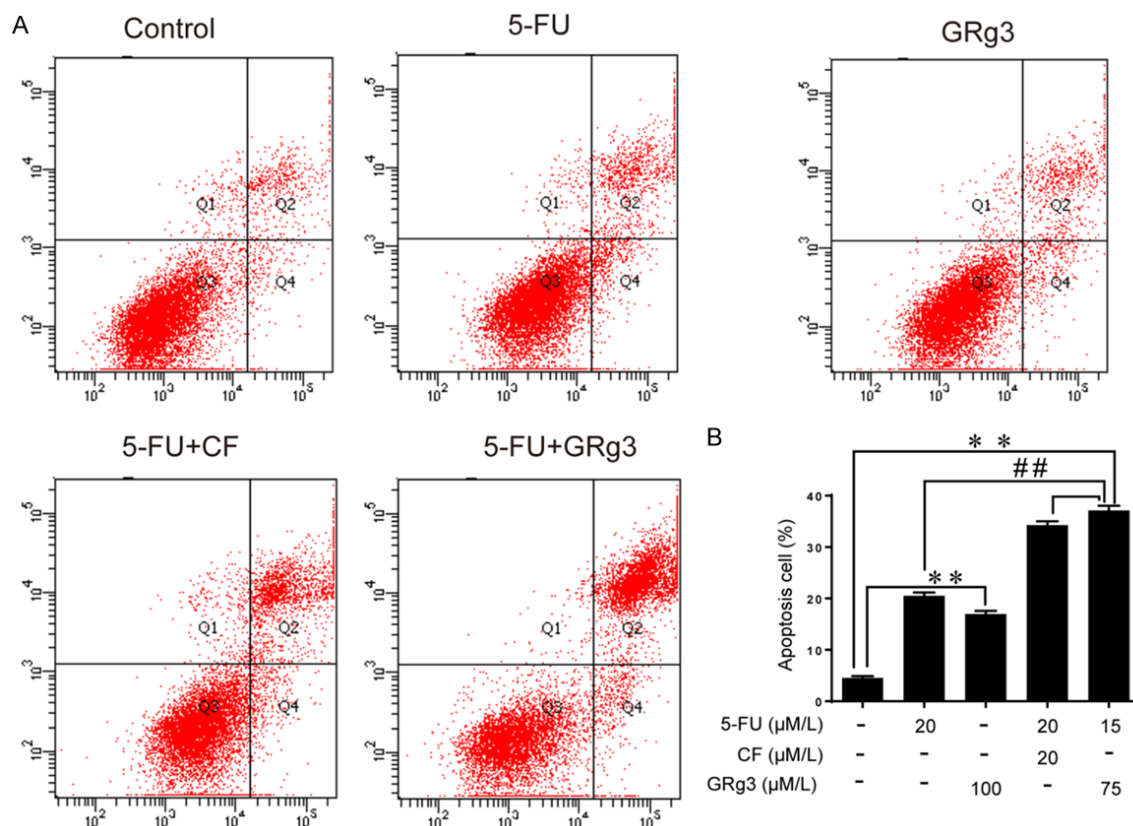
Figure 4. Cell apoptosis was determined by Annexin V-FITC/PI staining. A. HCT-116 cells were treated with 20 μM 5-FU, 100 μM GRg₃, 20 μM 5-FU + 20 μM CF or 15 μM 5-FU + 75 μM GRg₃ for 48 h. Apoptosis was detected by Annexin V-FITC/PI staining followed by Flow cytometry analysis. B. Quantitative analysis of apoptosis cells in all groups. All data are presented as mean ± s.e.m. (n = 3). **P < 0.05, **P < 0.01, compared with control. #P < 0.05, ##P < 0.01, compared with 5-FU.

5-FU + 20 μM CF or 15 μM 5-FU + 75 μM GRg₃ for 48 h. Then treated cells were harvested and disposed of as following steps: washed three times with cold 1 × PBS, cells were fixed gently with 70% ice-ethanol at 4°C stay overnight, washed twice with cold 1 × PBS, treated with 10% Triton X-100 for 5 min on an ice bath. Cells were resuspended in 500 μl of PBS containing 50 mg/ml PI and 100 mg/ml RNase A. Then cells were incubated in a dark room for 30 min at room temperature. At least 10,000 cells were detected by Flow cytometry. The cell cycle distribution was analyzed by the Modfit software.

Western bolt analysis

Cells were treated with 20 μM 5-FU, 100 μM GRg₃, 20 μM 5-F + 20 μM CF or 15 μM 5-FU + 75 μM GRg₃ for 48 h. Whole-cell lysates (50 μg) were prepared and separated by 10%

SDS-PAGE. And then proteins were transferred to nitrocellulose membrane by semi-dry (Bio-Rad). The membrane was blocked with 5% milk (w/v) at room temperature for 1 hour, and then incubated at 4°C overnight with primary antibodies (1:1000). Following 1 × PBST washing, the membranes were incubated with secondary antibody (1:7000) in the dark at room temperature for 2 h and then exposure at the Odyssey Infrared Imaging System (LI-COR, U.S.).

Statistical analysis

All data are presented as the mean ± sem from parallel experiments performed in triplicate, unless otherwise indicated. All comparisons in the data were performed using the Student's T-test and were considered statistically significant at P < 0.05 and P < 0.01. All analyses were performed using SPSS software version 19.0.
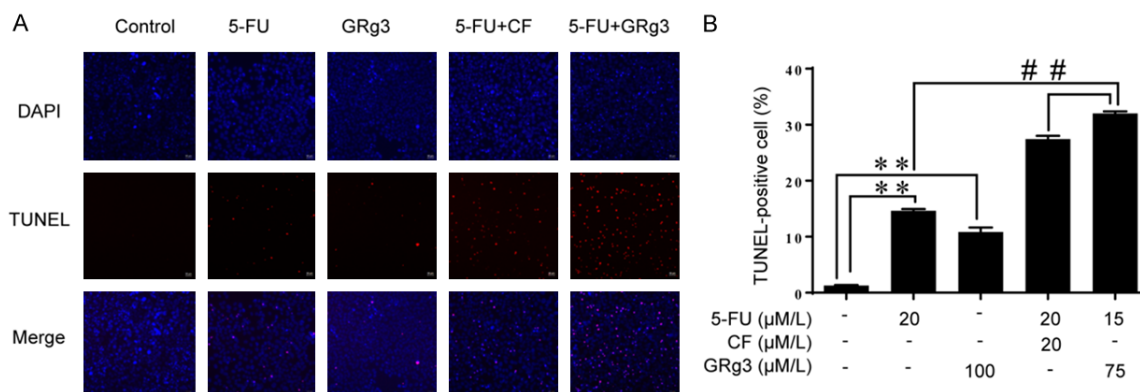
Figure 5. Apoptosis of HCT-116 cells were determined by TUNEL assay. A. The apoptosis features were accessed by observing the DAPI stained TUNEL-positive cells number counted in a given area. B. Quantitative analysis of the ratio of apoptosis cells in all groups. All data are presented as mean ± s.e.m. (n = 3). *P < 0.05, **P < 0.01, compared with control. #P < 0.05, ##P < 0.01, compared with 5-FU.

Results

5-FU and GRg₃ synergistically inhibit the growth of HCT-116 cells in vitro

After exposure to various concentrates of 5-FU (10, 20, 30, 40, 50 μM), GRg$_3$ (5, 25, 50, 75, 100 μM), 20 μM 5-FU + 20 μM CF or 15 μM 5-FU + GRg$_3$ (5, 25, 50, 75, 100 μM) for 48 h, their growth inhibitory effect on HCT-116 cells were determined by MTT assay. A dose-dependent inhibitive effect on cell growth was observed. As shown in **Figure 2A**, the IC$_{50}$ of 5-FU or GRg$_3$ was 25±5.47 or 111.4±6.9 μM, respectively. Importantly, the combination of 5-FU (15 μM) with GRg$_3$ in various concentration (5, 25, 50, 75, 100 μM) induced cytotoxicity (**Figure 2A**), and the IC$_{50}$ of GRg$_3$ modulated by 15 μM 5-FU was 18.6±2.1 μM. Moreover, GRg$_3$ in combination with 5-FU, compared with agents treated alone, augmented cytotoxicity (##P < 0.01), providing additional evidences for the synergism. In addition, co-treatment with 15 μM 5-FU plus 75 μM GRg$_3$ could approach an equivalent viability inhibitory effect in comparison with combination of 20 μM 5-FU plus 20 μM CF (P > 0.05) (**Figure 2B**). The CI value was determined by using CompuSy software. CI < 1 indicates synergism, CI > 1 indicates antagonism, CI = 1 indicates additive effect. Our Combination index analysis showed that 15 μM 5-FU combined with 5 μM GRg$_3$, the CI value = 1; 15 μM 5-FU combined with higher doses GRg$_3$, the CI value < 1 (**Figure 2C**). Notably, when 5-FU (15 μM) was combined with GRg$_3$ at a concentration higher than 5 μM, all of the points in isobologram analysis below the diago-

nal (**Figure 2D**), implying that the use of GRg$_3$ and 5-FU treatment for HCT-116 cells can lead to synergizes.

Effect of Ki67 expression on cell proliferation

Immunofluorescence staining of Ki67 was performed to investigate the effect of 20 μM 5-FU, 100 μM GRg$_3$, 20 μM 5-FU + 20 μM CF or 15 μM 5-FU + 75 μM GRg$_3$ in HCT-116 cells proliferation. The decrease of Ki67 expression was observed in both one-drug groups and co-treatment groups (**Figure 3A**). The ratio of Ki67 positive cells decreased to 30.3±0.75%, 36.6± 1.01%, respectively, after treat individually with 20 μM 5-FU or 100 μM GRg$_3$ for 48 h (**Figure 3B**). Significantly lower expression of Ki67 was observed in 5-FU + GRg$_3$ group (14.8±0.82%), compared with control group (49.8±1.5%, **P < 0.01). Importantly, when 15 μM 5-FU combined with 75 μM GRg$_3$ or 20 μM 5-FU combined with 20 μM CF, the expression of Ki67 decreased to 14.8±0.82% and 16.6±0.74%, which are significantly lower compared with 5-FU individual group (##P < 0.01). These results are consistent with the MTT assay, which firmly validated combination of 5-FU and GRg$_3$ synergistic inhibition on HCT-116 cells proliferation.

5-FU and GRg₃ induce HCT-116 cells apoptosis

Annexin V-FITC/PI staining was performed to investigate the apoptosis effect of 20 μM 5-FU, 100 μM GRg$_3$, 20 μM 5-FU + 20 μM CF or 15 μM 5-FU + 75 μM GRg$_3$ on HCT-116 cells. Compared to the control group (4.52±0.37%), 5-FU or GRg$_3$ single group increased apoptosis to
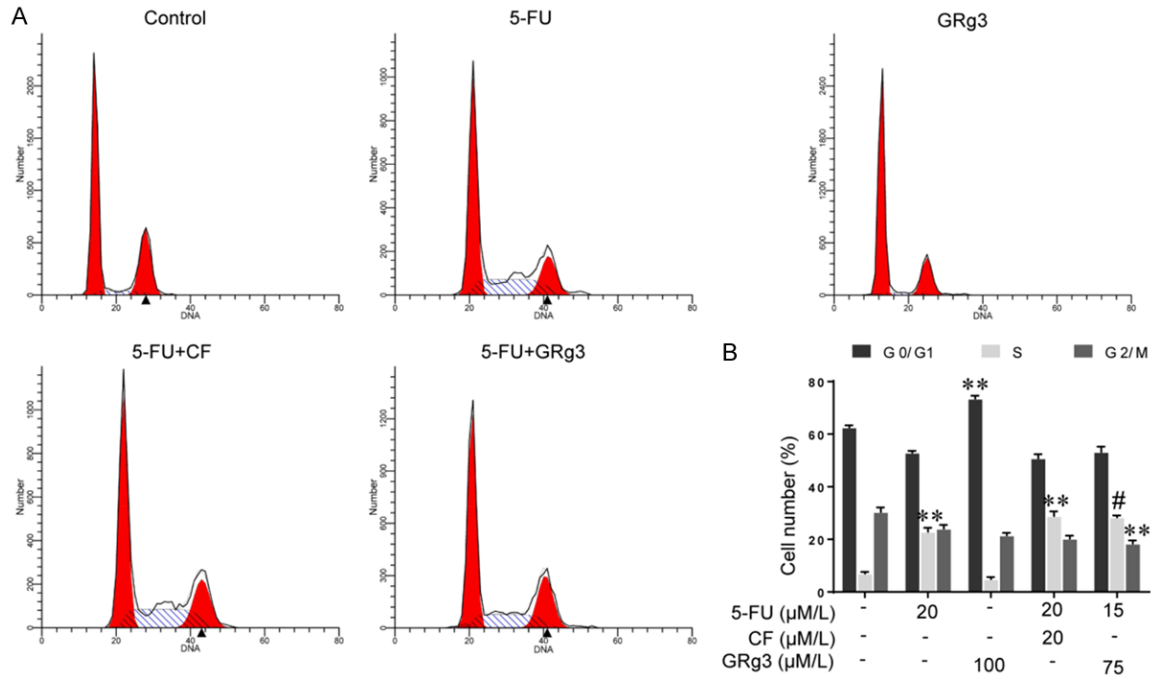
Figure 6. Effect of 5-FU and GRg$_3$ on cell cycle distribution. A. Changes in the cell cycle distribution after 48 h of treatment with 20 μM 5-FU, 100 μM GRg$_3$, 20 μM 5-FU + 20 μM CF or 15 μM 5-FU + 75 μM GRg$_3$. B. Quantitative analysis of cell cycle distribution in all groups. All data are presented as mean ± s.e.m. (n = 3). $^*P < 0.05$, $^{**}P < 0.01$, compared with control. $^\#P < 0.05$, $^{\#\#}P < 0.01$, compared with 5-FU.

20.6±0.61% or 16.9±0.58%, respectively ($^{**}P < 0.01$), compared with control. When 5-FU was combined with GRg$_3$, the percentage of apoptotic cells increased to 37.1±0.93%, which promoted apoptosis compared with control group ($^{**}P < 0.01$) and the combined effects were stronger than the effects of 5-FU ($^{\#\#}P < 0.01$) alone. No significant difference was found between 5-FU + GRg$_3$ group (37.1±0.93%) and 5-FU + CF group (34.2±0.72%) (**Figure 4**). Thus, this result suggested that the cell proliferation inhibition of combined 5-FU and GRg$_3$ may be related to the apoptotic induction.

5-FU and GRg$_3$ Induce morphological changes in HCT-116 cells

TUNEL staining was performed to detect the fragmented DNA in cells undergoing apoptosis. The observed changes in apoptotic cells detected by fluorescence microscope are shown in **Figure 5A**, the treatment group induced formation of apoptotic bodies, condensed DNA and other morphological changes while slightly blue and homogeneous cells were observed in control group. Cells were treated with 20 μM 5-FU, 100 μM GRg$_3$, 20 μM 5-FU + 20 μM CF or 15 μM 5-FU + 75 μM GRg$_3$ for 48 h, the cor-

responding quantities of apoptosis cell were 14.1±0.37%, 10.8±0.79%, 28.5±0.6%, 33.6± 0.8%. The above results showed that combination treatment of 15 μM 5-FU and 75 μM GRg$_3$ for 48 h caused the significantly increase in the level of apoptotic cells with red-blue fluorescence characteristic of TUNEL positive cells, compared with 5-FU group ($^{\#\#}P < 0.01$) (**Figure 5B**). There was no significant difference between 5-FU + CF (28.5±0.6%) group and 5-FU + GRg$_3$ (33.6±0.8%) group (**Figure 5B**).

5-FU and GRg$_3$ synergistically induce cell cycle arrest in HCT-116 cells

Flow cytometry was used to detect the effect of GRg$_3$ or 5-FU on cell cycle distribution of HCT-116 cells. Cells were incubated with 20 μM 5-FU, 100 μM GRg$_3$, 20 μM 5-FU + 20 μM CF or 15 μM 5-FU + 75 μM GRg$_3$ for 48 h and their effect on cell cycle distribution was studied. As shown in **Figure 6A**, GRg$_3$ treatment for 48 h induced a significant (12.4±0.94%, $^{**}P < 0.01$) increment of cell number in G$_1$ phase of HCT-116 cells, whereas 5-FU treatment induced S phase arrest (19.2±1.4%, $^{**}P < 0.01$). Following exposure to 75 μM of GRg$_3$ and 15 μM of 5-FU for 48 h, the percentage of HCT-116 cells at
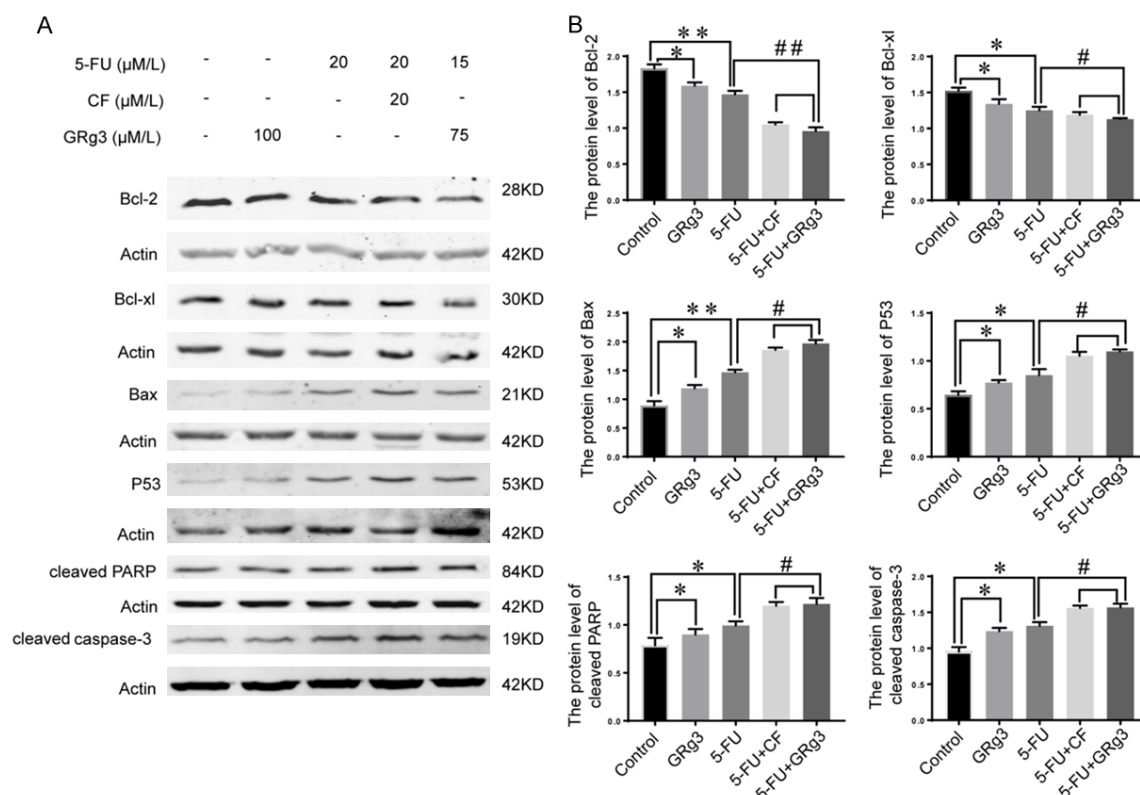
Figure 7. A. Cells were treated with 5-FU, GRg₃, 5-FU + CF and 5-FU + GRg₃ for 48 h at indicated doses, then whole cell lysates were prepared and analyzed by western blot using antibodies against Bcl-2, Bcl-xl, Bax, P53, cleaved caspase-3, cleaved PARP. B. The results were quantified by Densitometic analysis. All data are presented as mean ± s.e.m. (n = 3). *P < 0.05, **P < 0.01, compared with control. #P < 0.05, ##P < 0.01, compared with 5-FU.

the S phase of the cell cycle increased to 26.7%±1.89%, compared with those exposed only to 5-FU (#P < 0.05). Following exposure to 75 µM of GRg₃ and 15 µM of 5-FU for 48 h, the percentage of G₂/M population of cells was significantly reduced (15.1±1.84%), compared with the control group (31.3±0.76%) (**P < 0.01) (**Figure 6B**). Similarly, treatment with 5-FU + CF also significantly increased cell cycle arrest in the S phase (28.9±1.73%, **P < 0.01) alone with the reduction of cells in G₂/M phases, compared with control group. There was no significant difference between 5-FU + CF group and 5-FU + GRg₃ group. These results indicated that 5-FU and GRg₃ together exhibit greater cell cycle arrest in the S and G₁/G₀ than when used alone.

Regulatory mechanisms of GRg₃ and 5-FU induced apoptosis on HCT-116 cells

To determine the underlying mechanisms of above-mentioned findings, the influence of 5-FU or GRg₃ on apoptosis-relate proteins were further investigated by western blot assay. The highly decreased expression of Bcl-2 and Bcl-xl was observed (**Figure 7**) in the treatment of 20 µM 5-FU, 100 µM GRg₃ (**P < 0.01), whereas the cells treated with 15 µM 5-FU + 75 µM GRg₃ or 20 µM 5-FU + 20 µM CF showed a significant reduction when compared to 5-FU group (#P < 0.05). In contrast, simultaneous treatment of HCT-116 cells with 5-FU and GRg₃ increased significantly the level of P53, Bax, cleaved PARP and caspase-3 when compared to control group (**P < 0.01). Additionally all combinations significantly increased the level of P53, Bax, cleaved PARP and caspase-3 compared with 5-FU group (#P < 0.05). There have no significant difference between 5-FU + CF group and 5-FU + GRg₃ group. These results suggested that GRg₃ regulated apoptosis-relate protein expression and induced apoptosis by an intrinsic pathway, which is mediated by mitochondria manner.

Discussion

Anticancer and natural colon-targeting features of GRg_3 have prompted us whether for CRC treatment to combine it with 5-FU (a classic chemotherapeutic agent used for the treatment of CRC), there are many advantages, including delivery of lower dose agents with lower toxicity, and increased patient tolerance. Our study was designed to investigate the combination of 5-FU and GRg_3 as a possible preventive and/or treatment strategy for CRC. We determined the effect of the agents alone and in combination on the growth, apoptosis, cell cycle, proliferation markers and protein expression of specific proteins involved in CRC regulation.

Our present findings showed that GRg_3 can significantly augment the anticancer efficacy of 5-FU in HCT-116 cells in vitro by the cell viability and proliferation assays. The results of CI analysis indicated that GRg_3 was the favorable drug for use in combination with 5-FU. Further, Immunofluorescent staining also indicated that Ki67, the marker of tumor proliferation, was significantly reduced by GRg_3 combination with low dose 5-FU. Notably, our initial in vitro study clearly indicated that the ratio of the growth inhibition of the 15 μM 5-FU + 75 μM GRg_3 group is similar to 20 μM 5-FU + 20 μM CF group. For the 5-FU + CF regimen has been used as standard therapy for CRC [33], our results prompt that the Rg_3-based combination 5-FU may be a promising strategy for CRC treatment. To our knowledge, this is the first report of such an important effect of GRg_3.

In order to understand the mechanisms that lead to synergism between 5-FU and GRg_3 in HCT-116 cells, we investigated the role of apoptosis and cell cycle pathways in the enhanced anti-proliferative effects observed with 5-FU dosed alongside GRg_3.

In accordance with the cell viability and proliferation assays, combined treatment resulted in a significant decrease in the expression of anti-apoptotic Bcl-2, Bcl-xl and increased expression of pro-apoptotic proteins Bax. Furthermore, Annexin V-FITC/PI staining and TUNEL assay analysis also demonstrated that GRg_3 combined with 5-FU dramatically promoted apoptosis on HCT-116 cells, while little apoptosis in the control group. Previous reports suggest that GRg_3 and 5-FU induce apoptosis by regulation of Bcl-2 and Bax and inhibit cell cycle by inhibiting P53 [34-37]. Our results indicated that GRg_3 further enhanced 5-FU's ability to induce apoptosis.

P53 is a tightly regulated transcription factor that induces cell cycle arrest or apoptosis in response to cellular stress [38]. Furthermore, P53 has the ability to activate the transcription of various pro-apoptotic genes, including those encoding members of the Bcl-2 family [39]. By Western blot, the expression of P53 in 5-FU + GRg_3 treated cells is more increased than in 5-FU or GRg_3 treated alone cells. By Flow cytometry, the percentage of cells in G_0/G_1 and S phase of 5-FU + GRg_3 treated cells was significantly increased than of 5-FU treated alone cells. These results are consistent with previous reports, which P53 not only induces G_1 cell cycle arrest, but it is also described to act at the G_2/M checkpoint, preventing cells from entering mitosis if DNA damage is found [40].

Caspase are the key proteins that modulate the apoptotic response. Caspase-3 is a key executioner of apoptosis, which is activated by an initiator caspase such as caspase-9. These activated caspases cleave many cellular substrates, ultimately leading to cell death [41]. The presence of cleaved PARP is one of the most used biomarkers for the detection of apoptosis [42]. Moreover, PARP is a substrate of caspase-3 and its cleavage into two fragments has been considered to be indicative of functional caspase activation [43]. Consistent with their effects on apoptosis, the combined treatment up-regulated the expression of the cleaved caspase-3 and the cleaved PARP in HCT-116 cells, indicating GRg_3 promote apoptosis and chemo-sensitivity to 5-FU through a mitochondria-dependent apoptosis cascade.

Taken together, these studies demonstrated that GRg_3 promoted cytotoxicity and apoptotic effect of 5-FU on HCT-116 cells. The mechanism of synergism is probably that combined treatment up-regulates P53 proteins, which in turn increases Bax, decreases Bcl-2 and Bcl-xl, activates caspase-3, cleaves PARP, and induces apoptosis. Therefore, our results imply that combining 5-FU and GRg_3 is a very attractive modulation strategy for 5-FU chemotherapy in clinical CRC treatment. Further in vivo and clini-

cal studies are warranted to evaluate the therapeutic potential of 5-FU combined with GRg₃ for CRC treatment.

Disclosure of conflict of interest

None.

Address correspondence to: De-Xi Guo, Department of Pharmacy, Gansu Provincial People's Hospital, 204 Donggang West Road, Lanzhou 730000, PR China. Tel: +86-13893408199; E-mail: yxl1668@vip.163.com

References

[1] Lahti S, Ludwig JM, Xing M, Sun L, Zeng D, Kim HS. In vitro biologic efficacy of sunitinib drug-eluting beads on human colorectal and hepatocellular carcinoma-A pilot study. PLoS One 2017; 12: e0174539.

[2] Redondo Blanco S, Fernández J, Gutiérrez Del-Río I, Villar CJ, Lombó F. New insights toward colorectal cancer chemotherapy using natural bioactive compounds. Front Pharmacol 2017; 8: 1-22.

[3] Klubes P, Connelly K, Cerna I, Mandel HG. Effects of 5-fluorouracil on 5-fluorodeoxyuridine 5'-monophosphate and 2-deoxyuridine 5'-monophosphate pools, and DNA synthesis in solid mouse L1210 and rat Walker 256 tumors. Cancer Res 1978; 38: 2325-2331.

[4] Giles GR, Woodhouse L, Finan PJ, Chisholm EM. Incorporation of intermediary products of 5-FU anabolism into colorectal cancer. Gut 1986; 27: 176-181

[5] Van Der Wilt CL, Pinedo HM, Smid K, Cloos J, Noordhuis P, Peters GJ. Effect of folinic acid on fluorouracil activity and expression of thymidylate synthase. Semin Oncol 1992; 19: 16-25.

[6] Morris MJ, Newland RC, Pheils MT, Macpherson JG. Hepatic metastases from colorectal carcinoma: an analysis of survival rates and histopathology. Aust N Z J Surg 1977; 47: 365-368.

[7] Shi DB, Li XX, Zheng HT, Li DW, Cai GX, Peng JJ, Gu WL, Guan ZQ, Xu Y, Cai SJ. Icariin-mediated inhibition of NF-kappaB activity enhances the in vitro and in vivo antitumour effect of 5-fluorouracil in colorectal cancer. Cell Biochem Biophys 2014; 69: 523-530.

[8] Tolba MF, Abdel Rahman SZ. Pterostilbine, an active component of blueberries, sensitizes colon cancer cells to 5-fluorouracil cytotoxicity. Sci Rep 2015; 5: 1-12.

[9] Einbond LS, Negrin A, Kulakowski DM, Wu HA, Antonetti V, Jalees F, Law W, Roller M, Redenti S, Kennelly EJ, Balick MJ. Traditional preparations of kava (Piper methysticum) inhibit the growth of human colon cancer cells in vitro. Phytomedicine 2017; 24: 1-13.

[10] Zhao Q, Wang J, Zou MJ, Hu R, Zhao L, Qiang L, Rong JJ, You QD, Guo QL. Wogonin potentiates the antitumor effects of low dose 5-fluorouracil against gastric cancer through induction of apoptosis by down-regulation of NF-kappaB and regulation of its metabolism. Toxicol Lett 2010; 197: 201-210.

[11] Hu B, Wang SS, Du Q. Traditional Chinese medicine for prevention and treatment of hepatocarcinoma: from bench to bedside. World J Hepatol 2015; 7: 1209-1232.

[12] Chang L, Huo BJ, Lv YL, Wang YD, Liu W. Ginsenoside Rg3 enhances the inhibitory effects of chemotherapy on esophageal squamous cell carcinoma in mice. Mol Clin Oncol 2014; 2: 1043-1046.

[13] Kim H, Hong MK, Choi H, Moon HS, Lee HJ. Chemopreventive effects of Korean Red Ginseng extract on rat hepatocarcinogenesis. J Cancer 2015; 6: 1-8.

[14] Chen SH, Wang ZJ, Huang Y, O'barr SA, Wong RA, Yeung S, Chow MS. Ginseng and anticancer drug combination to improve cancer chemotherapy: a critical review. Evid Based Complement Alternat Med 2014; 2014: 168940.

[15] Seo EY, Kim WK. Red ginseng extract reduced metastasis of colon cancer cells in vitro and in vivo. J Ginseng Res 2011; 35: 315-324.

[16] Xie Q, Wen H, Zhang Q, Zhou W, Lin X, Xie D, Liu Y. Inhibiting PI3K-AKt signaling pathway is involved in antitumor effects of ginsenoside Rg3 in lung cancer cell. Biomed Pharmacother 2017; 85: 16-21.

[17] Li ZJ, Zhu H, Ma BY, Zhao F, Mao SH, Liu TG, He JP, Deng LI, Yi C, Huang Y. Inhibitory effect of Bifidobacterium infantis-mediated sKDR prokaryotic expression system on angiogenesis and growth of Lewis lung cancer in mice. BMC Cancer 2012; 12: 155-166.

[18] Zeng DF, Wang JL, Kong PY, Chang C, Li JP, Li JL. Ginsenoside Rg3 inhibits HIF-1α and VEGF expression in patient with acute leukemia via inhibiting the activation of PI3K/Akt and ERK1/2 pathways. Int J Clin Exp Pathol 2014; 7: 2172-2178.

[19] Sun HQ, Zhou ZY. Effect of ginsenoside-Rg3 on the expression of VEGF and TNF-α in retina with diabetic rats. Int J Ophthalmol 2010; 3: 220-223.

[20] Sun HY, Lee JH, Han YS, Yoon YM, Yun CW, Kim JH, Song YS, Lee SH. Pivotal roles of ginsenoside Rg3 in tumor apoptosis through regulation of reactive oxygen species. Anticancer Res 2016; 36: 4647-4654.

[21] Kim BM, Kim DH, Park JH, Surh YJ, Na HK. Ginsenoside Rg3 inhibits constitutive activation of NF-κB signaling in human breast cancer (MDA-MB-231) cells: ERK and Akt as potential upstream targets. J Cancer Prev 2014; 19: 23-30.

[22] Kim BJ, Nah SY, Jeon JH, So I, Kim SJ. Transient receptor potential melastatin 7 channels are involved in ginsenoside Rg3-induced apoptosis in gastric cancer cells. Basic Clin Pharmacol Toxicol 2011; 109: 233-239.

[23] Zhang X, Chen K, Wei B, Liu X, Lei Z, Bai X. Ginsenosides Rg3 attenuates glucocorticoid-induced osteoporosis through regulating BMP-2/BMPR1A/Runx2 signaling pathway. Chem Biol Interact 2016; 256: 188-197.

[24] Cui XL, Jin Y, Poudyal D, Chumanevich AA, Davis T, Windust A, Hofseth A, Wu W, Habiger J, Pena E, Wood P, Nagarkatti M, Nagarkatti PS, Hofseth L. Mechanistic insight into the ability of American ginseng to suppress colon cancer associated with colitis. Carcinogenesis 2010; 31: 1734-1741.

[25] Dougherty U, Mustafi R, Wang Y, Musch MW, Wang CZ, Konda VJ, Kulkarni A, Hart J, Dawson G, Kim KE, Yuan CS, Chang EB, Bissonnette M. American ginseng suppresses western diet-promoted tumorigenesis in model of inflammation-associated colon cancer: role of EGFR. BMC Complement Altern Med 2011; 11: 111-122.

[26] Li BH, Wang CZ, He TC, Yuan CS, Du W. Antioxidants potentiate American ginseng-induced killing of colorectal cancer cells. Cancer Lett 2010; 289: 62-70.

[27] Qi LW, Wang CZ, Yuan CS. Ginsenosides from American ginseng: chemical and pharmacological diversity. Phytochemistry 2011; 72: 689-699.

[28] Voruganti S, Qin JJ, Sarkar S, Nag S, Walbi IA, Wang S, Zhao YQ, Wang W, Zhang RW. Oral nano-delivery of anticancer ginsenoside 25-OCH(3)-PPD, a natural inhibitor of the MDM2 oncogene: nanoparticle preparation, characterization, in vitro and in vivo anti-prostate cancer activity, and mechanisms of action. Oncotarget 2015; 6: 21379-21394.

[29] Zhang X, Zhang D, Xu J, Gu J, Zhao Y. Determination of 25-OH-PPD in rat plasma by high-performance liquid chromatography-mass spectrometry and its application in rat pharmacokinetic studies. J Chromatogr B Analyt Technol Biomed Life Sci 2007; 858: 65-70.

[30] Qian T, Cai Z, Wong RN, Mak NK, Jiang ZH. In vivo rat metabolism and pharmacokinetic studies of ginsenoside Rg3. J Chromatogr B Analyt Technol Biomed Life Sci 2005; 816: 223-232.

[31] Liang Y, Zhou Y, Zhang J, Rao T, Zhou L, Xing R, Wang Q, Fu H, Hao K, Xie L, Wang G. Pharmacokinetic compatibility of ginsenosides and schisandra lignans in shengmai-san: from the perspective of p-glycoprotein. PLoS One 2014; 9: e98717.

[32] Zhou X, Seto SW, Chang D, Kiat H, Razmovski-Naumovski V, Chan K, Bensoussan A. Synergistic effects of Chinese herbal medicine: a comprehensive review of methodology and current research. Front Pharmacol 2016; 7: 201-215.

[33] Pfeiffer P, Mortensen JP, Bjerregaard B, Eckhoff L, Schonnemann K, Sandberg E, Aabo K, Jakobsen A. Patient preference for oral or intravenous chemotherapy: a randomised crossover trial comparing capecitabine and nordic fluorouracil/leucovorin in patients with colorectal cancer. Eur J Cancer 2006; 42: 2738-2743.

[34] Chuang JC, Sheu GT, Wang PC, Liao FT, Liu WS, Huang CF, Tseng MH, Wu MF. Docetaxel and 5-fluorouracil induce human p53 tumor suppressor gene transcription via a short sequence at core promoter element. Toxicol In Vitro 2012; 26: 678-685.

[35] Park HM, Kim SJ, Kim JS, Kang HS. Reactive oxygen species mediated ginsenoside Rg3- and Rh2-induced apoptosis in hepatoma cells through mitochondrial signaling pathways. Food Chem Toxicol 2012; 50: 2736-2741.

[36] Yu DF, Wu FR, Liu Y, Liu H, Xia Q. Bcl-2 gene silence enhances the sensitivity toward 5-Fluorouracil in gastric adenocarcinoma cells. Biomed Pharmacother 2013; 67: 615-619.

[37] Yuan Z, Jiang H, Zhu X, Liu X, Li J. Ginsenoside Rg3 promotes cytotoxicity of Paclitaxel through inhibiting NF-kappaB signaling and regulating Bax/Bcl-2 expression on triple-negative breast cancer. Biomed Pharmacother 2017; 89: 227-232.

[38] Yeh YT, Yeh H, Su SH, Lin JS, Lee KJ, Shyu HW, Chen ZF, Huang SY, Su SJ. Phenethyl isothiocyanate induces DNA damage-associated G2/M arrest and subsequent apoptosis in oral cancer cells with varying p53 mutations. Free Radic Biol Med 2014; 74: 1-13.

[39] Roos WP, Kaina B. DNA damage-induced cell death: from specific DNA lesions to the DNA damage response and apoptosis. Cancer Lett 2013; 332: 237-248.

[40] Taylor WR, Stark GR. Regulation of the G2/M transition by p53. Oncogene 2001; 20: 1803-1815.

[41] Samejima K, Villa P, Earnshaw WC. Role of factors downstream of caspases in nuclear disassembly during apoptotic execution. Philos Trans R Soc Lond B Biol Sci 1999; 354: 1591-1599.

[42] Vizetto Duarte C, Custodio L, Gangadhar KN, Lago JH, Dias C, Matos AM, Neng N, Nogueira JM, Barreira L, Albericio F, Rauter AP, Varela J. Isololiolide, a carotenoid metabolite isolated from the brown alga Cystoseira tamariscifolia, is cytotoxic and able to induce apoptosis in hepatocarcinoma cells through caspase-3 activation, decreased Bcl-2 levels, increased p53 expression and PARP cleavage. Phytomedicine 2016; 23: 550-557.

[43] Prabhakaran K, Li L, Borowitz JL, Isom GE. Caspase inhibition switches the mode of cell death induced by cyanide by enhancing reactive oxygen species generation and PARP-1 activation. Toxicol Appl Pharmacol 2004; 195: 194-202.